13.472J/1.128J/2.158J/16.940J
COMPUTATIONAL GEOMETRY

Lecture 9

N. M. Patrikalakis

Massachusetts Institute of Technology
Cambridge, MA 02139-4307, USA

Contents

Lecture 9

Blending Surfaces

9.1 Examples and motivation

Blending surfaces, providing a smooth connection between various primary or functional surfaces, are very common in CAD. Examples include blending surfaces between:

- Fuselage and wings of airplanes
- Propeller or turbine blade and hub
- Bulbous bow and ship hull
- Primary faces of solid models.

Blending (or filleting) surfaces are also byproducts of manufacturing processes such as NC milling with a ball or disk cutter.

As a result of continuity conditions, blending surfaces are of higher order, or involve a more complex formulation than the underlying surfaces to be joined. For a detailed review, see Woodwark [15], and Hoschek and Lasser [9] (chapter 14).

Example

Join bicubic patches along arbitrary cubic linkage curves in parametric space (see Figure 9.1).

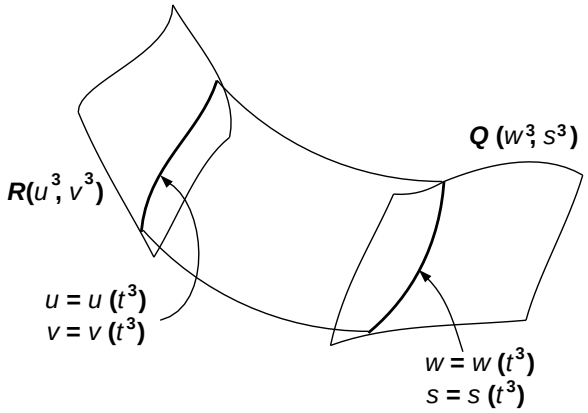

Figure 9.1: Bicubic patches joined along arbitrary cubic linkage curves.

Linkage curve 1 is:

$$\mathbf{R}_1(t) \equiv \mathbf{R}(t) = \mathbf{R}(u^3, v^3) \equiv \mathbf{R}(t^{18}), \text{ if } u = u(t^3), v = v(t^3) \tag{9.1}$$

Similarly, curve 2 is:

$$\mathbf{R}_2(t) \equiv \mathbf{Q}(t) = \mathbf{Q}(w^3, s^3) \equiv \mathbf{Q}(t^{18}), \text{ if } w = w(t^3), s = s(t^3) \tag{9.2}$$

So position continuity alone requires a high degree surface in the t parameter direction (of degree 18 in this example). High degree surfaces are expensive to evaluate (e.g. the de Casteljau or Cox-de Boor algorithms have quadratic complexity in the degree of the curve or surface), may lead to greater inaccuracy of evaluation (as the degree increases), and are difficult to process in a solid modeling environment (e.g. through intersections). Consequently, researchers have developed:

- Approximations of blending surfaces with low order B-spline surfaces
- Procedural definitions of blending surfaces (e.g. "lofted" surfaces, generalized cylinders)

in order to reduce some of these problems.

9.2 Blending surface approximation in terms of B-splines

Let us consider two parametric surface patches $\mathbf{r}_{m_1n_1}(u,v)$, $\mathbf{r}_{m_2n_2}(x,y)$ and linkage curves $\mathbf{R}_1(t) = [u(t), v(t)]$, $\mathbf{R}_2(t) = [x(t), y(t)]$ defined in the parameter spaces of the two patches, respectively.

The unit normal to $\mathbf{R}_1$ that is tangent to the patch (see Figure 9.2):

$$\mathbf{r}_1(t) = \frac{\mathbf{N} \times \mathbf{S}_1}{|\mathbf{N} \times \mathbf{S}_1|} \left| \begin{array}{l} \\ u = u(t) \\ v = v(t) \end{array} \right. \tag{9.3}$$

where $\mathbf{N} = \mathbf{r}_u \times \mathbf{r}_v$ is the normal to the patch, and $\mathbf{S}_1 = \dot{u}(t)\mathbf{r}_u(u(t), v(t)) + \dot{v}(t)\mathbf{r}_v(u(t), v(t))$ where $\mathbf{r} = \mathbf{r}_{m_1n_1}(u, v)$. In general, $\mathbf{N}$ and $\mathbf{S_1}$ are high order polynomials. For example, when the patch is bicubic and the linkage curve is cubic in the parameter space, we have

$$\mathbf{N} \sim \mathbf{r}_u \times \mathbf{r}_v \sim u^2v^3u^3v^2 \sim u^5v^5 \sim t^{30}$$

$$\mathbf{S}_1 \sim \dot{u}\mathbf{r}_u \sim t^2u^2v^3 \sim t^2t^6t^9 \sim t^{17}$$

Next, we introduce bias functions $b_1(t), b_2(t)$ to control the shape of the blending surface and define:

$$\mathbf{q_1}(t) = b_1(t)\mathbf{r}_1(t) \tag{9.4}$$

$$\mathbf{q_2}(t) = b_2(t)\mathbf{r}_2(t) \tag{9.5}$$

to be used as parametric derivatives of the patch in the direction between the linkage curves. For details, see Bardis and Patrikalakis [1].

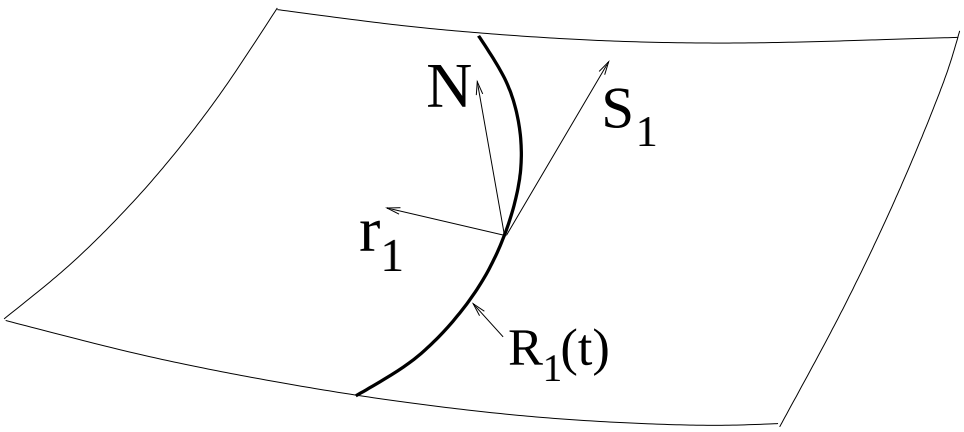

Figure 9.2: $\mathbf{N}$, $\mathbf{S}_1$ $\mathbf{r}_1$ frame

9.2.1 Blend construction through a procedural "lofted" surface

Here we use cubic Hermite polynomials as blending functions in the direction between the linkage curves:

$$\begin{aligned} H_1(w) &= 1 - 3w^2 + 2w^3 && (9.6)\\ H_2(w) &= 3w^2 - 2w^3 && (9.7)\\ H_3(w) &= w - 2w^2 + w^3 && (9.8)\\ H_4(w) &= w^3 - w^2 && (9.9) \end{aligned}$$

These obey the following boundary conditions:

$$\begin{aligned} H_1(0) = 1 \quad , \quad H_1(1) &= H_1'(0) = H_1'(1) = 0 && (9.10)\\ H_2(1) = 1 \quad , \quad H_2(0) &= H_2'(0) = H_2'(1) = 0 && (9.11)\\ H_3'(0) = 1 \quad , \quad H_3(0) &= H_3(1) = H_3'(1) = 0 && (9.12)\\ H_4'(1) = 1 \quad , \quad H_4(0) &= H_4'(0) = H_4(1) = 0 && (9.13) \end{aligned}$$

Then the blending surface is:

$$\mathbf{B}(w,t) = \mathbf{R}_1(t)H_1(w) + \mathbf{R}_2(t)H_2(w) + \mathbf{q}_1(t)H_3(w) + \mathbf{q}_2(t)H_4(w) \qquad (9.14)$$

where $\mathbf{R}_1, \mathbf{R}_2$ are evaluated using a composition mapping (due to high degree, explicit expressions are avoided, e.g. degree 18 for cubics), and $\mathbf{q}_1, \mathbf{q}_2$ are similarly evaluated procedurally (to avoid explicit expressions), given that:

$$\begin{aligned} \mathbf{r}_1 &\sim t^{47}/\sqrt{t^{47}} && (9.15)\\ \mathbf{q}_1 &\sim t^{50}/\sqrt{t^{47}} && (9.16) \end{aligned}$$

Next, we construct cubic B-spline approximations to $\mathbf{R}_1, \mathbf{R}_2, \mathbf{q}_1, \mathbf{q}_2$:

$$\begin{aligned} \mathbf{R}_1(t) &\cong \sum_{\ell=0}^{n} \mathbf{R}_\ell^{(1)} N_{\ell,4}(t) && (9.17)\\ \mathbf{R}_2(t) &\cong \sum_{\ell=0}^{n} \mathbf{R}_\ell^{(2)} N_{\ell,4}(t) && (9.18)\\ \mathbf{q}_1(t) &\cong \sum_{\ell=0}^{n} \mathbf{Q}_\ell^{(1)} N_{\ell,4}(t) && (9.19)\\ \mathbf{q}_2(t) &\cong \sum_{\ell=0}^{n} \mathbf{Q}_\ell^{(2)} N_{\ell,4}(t) && (9.20) \end{aligned}$$

where $N_{\ell,4}(t)$ are cubic non-uniform B-spline basis functions and the same knot vector and number of control points is used in all four equations.

This approximation involves a process for the insertion of knots until errors are less than specified tolerances for the previous four vector functions.

The equation for the resulting blending surface is:

$$\mathbf{B}(w,t) = \sum_{k=0}^{3}\sum_{\ell=0}^{n}\mathbf{B}_{k,\ell}\overbrace{B_{k,4}(w)}^{\text{Bézier}}\overbrace{N_{\ell,4}(t)}^{\substack{\text{Above}\\ \text{B-spline}}} \tag{9.21}$$

$$\mathbf{B}_w(w,t) = 3\sum_{\ell=0}^{n}\sum_{k=1}^{3}(\mathbf{B}_{k,\ell}-\mathbf{B}_{k-1,\ell})B_{k,3}(w)N_{\ell,4}(t) \tag{9.22}$$

From position and derivative continuity we get:

$$\mathbf{B}_{0,\ell} = \mathbf{R}_\ell^{(1)} \tag{9.23}$$

$$\mathbf{B}_{3,\ell} = \mathbf{R}_\ell^{(2)} \tag{9.24}$$

$$\mathbf{B}_{1,\ell} = \mathbf{R}_\ell^{(1)} + \mathbf{Q}_\ell^{(1)}/3 \tag{9.25}$$

$$\mathbf{B}_{2,\ell} = \mathbf{R}_\ell^{(2)} - \mathbf{Q}_\ell^{(2)}/3 \tag{9.26}$$

The disadvantage of approximation is the increase in data and the resulting storage requirements. The advantage is that the same class of functions is used which makes it easy to include in a geometric modeler and easy to transfer between CAD/CAM systems.

Special attention needs to be given to the correspondence of parametrization of linkage curves and this may necessitate reparametrization of linkage curves. See Bardis and Patrikalakis [1], and Hansmann [7] for more details on these issues.

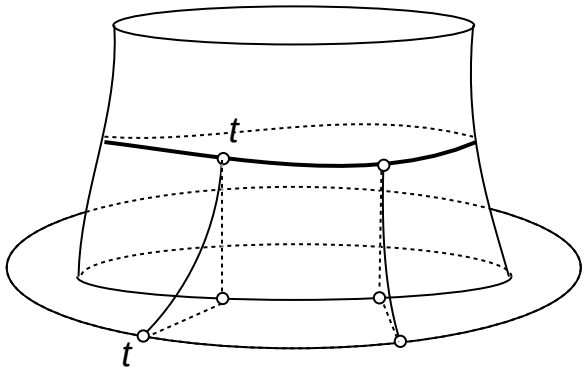

Figure 9.3: Blending surface cross-link curves.

9.3 Spherical and circular blending in terms of generalized cylinders

For a detailed reference on this topic, see Pegna [12].

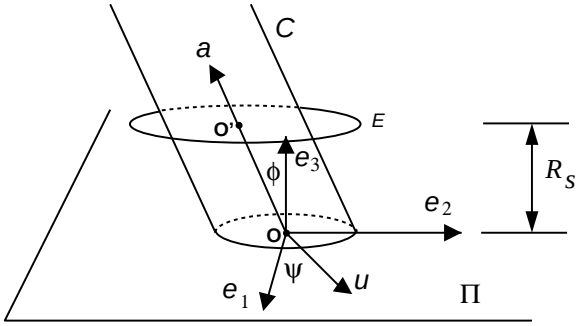

Figure 9.4: Model of milling via a spherical ball cutter (3-axis milling) or a disk cutter (5-axis).

The center of the sphere (or spherical cutter) moves on the intersection curve of the offsets of the plane Π and cylinder C of radius R_c by an offset amount equal to R_s, i.e. ellipse E (see Figure 9.4).

Let $\mathbf{a}$ be a unit vector along the cylinder axis, $\mathbf{e}_3$ a unit vector perpendicular to plane Π, and O the intersection of the cylinder axis and the plane. Also,

$$\mathbf{e}_1 = \frac{\mathbf{e}_3 \times \mathbf{a}}{|\mathbf{e}_3 \times \mathbf{a}|} \tag{9.27}$$

$$\mathbf{e}_2 = \mathbf{e}_3 \times \mathbf{e}_1 \tag{9.28}$$

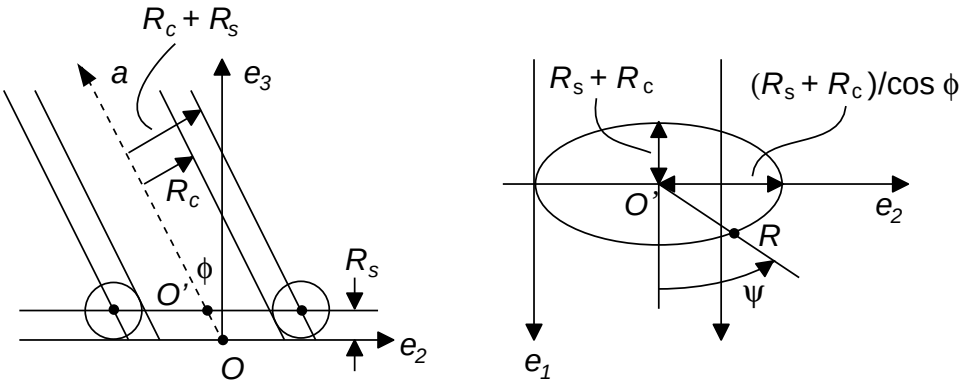

Figure 9.5: Definition of the ellipse.

Find the directrix E, an ellipse. The center of E is $[0, -R_s \tan\phi, R_s] = \mathbf{R}_{O'}$. The major axis is $(R_s + R_c)/\cos\phi$ along $\mathbf{e}_2$. The minor axis is $R_s + R_c$ in the direction parallel to $\mathbf{e}_1$.

$$\mathbf{a} = [0, -\sin\phi, \cos\phi] \tag{9.29}$$

- The equation of the ellipse is (see Figure 9.5):

$$\mathbf{R}(\psi) = \mathbf{R}_{O'} + \mathbf{e}_1(R_C + R_s)\cos\psi + \mathbf{e}_2\frac{R_c + R_s}{\cos\phi}\sin\psi \tag{9.30}$$

- The projection of the center of the sphere (or projection of the ellipse) on the plane is:

$$\mathbf{t}_p = (R_c + R_s)\cos\psi\mathbf{e}_1 + \left[\frac{R_c + R_s}{\cos\phi}\sin\psi - R_s\tan\phi\right]\mathbf{e}_2 \tag{9.31}$$

- $\mathbf{t}_c$: Projection of $\mathbf{R}$ (equation of the ellipse that is the center of the sphere) to the cylinder.

  $\mathbf{P}$: Projection of $\mathbf{R}$ onto the axis $\mathbf{a}$.

$$\mathbf{v} = \frac{\mathbf{P} - \mathbf{R}}{|\mathbf{P} - \mathbf{R}|} \quad \text{(unit normal)} \tag{9.32}$$

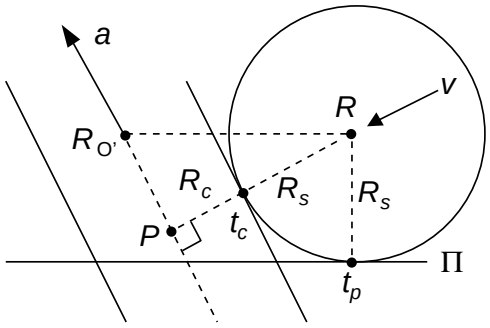

Figure 9.6: Side view.

Observe that:

$$\begin{aligned}
\mathbf{P} - \mathbf{R}_{O'} &= ((\mathbf{R} - \mathbf{R}_{O'})\cdot\mathbf{a})\mathbf{a} && (9.33)\\
&= \mathbf{a}(-1)\tan\phi\sin\psi(R_c + R_s) && (9.34)\\
\mathbf{P} - \mathbf{R} &= (\mathbf{P} - \mathbf{R}_{O'}) - (\mathbf{R} - \mathbf{R}_{O'}) && (9.35)\\
&= -(R_c + R_s)\tan\phi\sin\psi[0, -\sin\phi, \cos\phi] - && (9.36)\\
&\quad (R_c + R_s)[\cos\psi, \frac{\sin\psi}{\cos\phi}, 0] && (9.37)\\
\mathbf{P} - \mathbf{R} &= (R_c + R_s)[-\cos\psi, -\sin\psi\cos\phi, -\sin\phi\sin\psi] && (9.38)\\
\mathbf{v} &= \frac{\mathbf{P} - \mathbf{R}}{|\mathbf{P} - \mathbf{R}|} = -[\cos\psi, \sin\psi\cos\phi, \sin\phi\sin\psi] && (9.39)
\end{aligned}$$

Hence,

$$\mathbf{t}_c = \mathbf{R} + R_s\mathbf{v} \tag{9.40}$$

where

$$\mathbf{R}(\psi) = \left[(R_c + R_s)\cos\psi, \frac{R_c + R_s}{\cos\phi}\sin\psi - R_s\tan\phi, R_s\right] \tag{9.41}$$

$$\mathbf{t}_c = \left[R_c\cos\psi, \frac{R_c\sin\psi}{\cos\phi} + R_S\left(\frac{\sin\psi}{\cos\phi} - \tan\phi - \sin\phi\cos\phi\right), \right. \tag{9.42}$$

$$\left. R_s(1 - \sin\phi\sin\psi)\right]$$

which simplifies to

$$\mathbf{t}_c = \left[R_c\cos\psi, \frac{R_c\sin\psi}{\cos\phi} + R_s\tan\phi(\sin\psi\sin\phi - 1), R_s(1 - \sin\phi\sin\psi)\right] \tag{9.43}$$

Notice that $\mathbf{v}$ is in the normal plane to the directrix:

$$\mathbf{v}\cdot\mathbf{R}_\psi = 0 \tag{9.44}$$

where

$$\mathbf{R}_\psi = \left[-(R_c + R_s)\sin\psi, \frac{R_c + R_s}{\cos\phi}\cos\psi, 0\right] \tag{9.45}$$

Hence, the generatrix is the arc of a great circle of the sphere on the plane $\mathbf{t}_c - \mathbf{R}, \mathbf{t}_p - \mathbf{R}$ between $\mathbf{t}_c$ and $\mathbf{t}_p$. The angle of the arc is

$$\theta = \cos^{-1}(-\mathbf{e}_3\cdot\mathbf{v}) = \cos^{-1}(\sin\phi\sin\psi) \tag{9.46}$$

in the local $\mathbf{n}, \mathbf{b}$ system of the directrix.

$$\mathbf{q}(v,\psi) = R_s[\sin\theta v\mathbf{n} - \cos\theta v\mathbf{b}] \quad \text{for } v\in[0,1] \tag{9.47}$$

where

$$\mathbf{b} = \mathbf{e}_3 \tag{9.48}$$

$$\mathbf{t} = \frac{\mathbf{R}_\psi}{|\mathbf{R}_\psi|} \tag{9.49}$$

$$\mathbf{n} = \mathbf{e}_3\times\mathbf{t} \tag{9.50}$$

Setting $\psi = 2\pi u$ for $u\in[0,1]$, the blending surface is:

$$\mathbf{B}(u,v) = \mathbf{R}(\psi(u)) + \mathbf{q}(v,\psi(u)) \tag{9.51}$$

Note that the surface is *not* a rational polynomial surface.

This result generalizes to spherical blends of general surfaces. A schematic diagram of spherical blends of surfaces is shown in Figure 9.7. The implementation is procedural and involves intersections of offset surfaces [11, 10] to define the directrix and the projection of a point on a surface to define the generatrix [14].

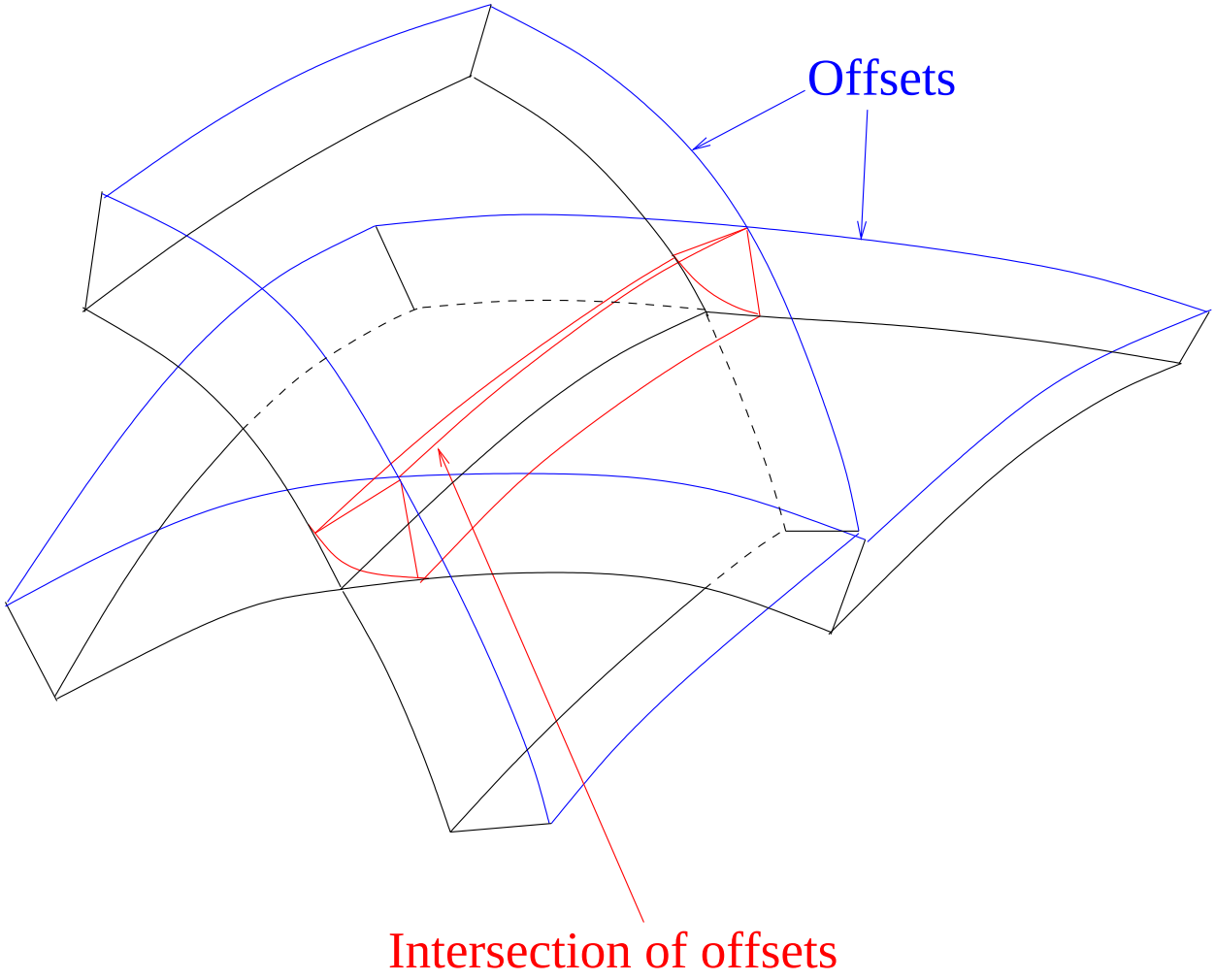

Figure 9.7: Spherical blends of surfaces

9.4 Blending of implicit algebraic surfaces

For a detailed reference, see Hoffmann and Hopcroft [8].

Given the implicit algebraic surfaces G, H defined as:

$$\left.\begin{array}{rcl} G(x,y,z) - s &=& 0 \\ H(x,y,z) - t &=& 0 \end{array}\right\} \text{potential surfaces} \tag{9.52}$$

define $f(s,t) = 0$, e.g:

$$\begin{aligned} f(s,t) &= b^2s^2 + a^2t^2 + a^2b^2 - 2ab^2s - 2a^2bt + 2\lambda st && (9.53)\\ f_s &= 2sb^2 - 2ab^2 + 2\lambda t && (9.54)\\ f_t &= 2ta^2 - 2ba^2 + 2\lambda s && (9.55)\\ \mathbf{n} &= (f_s, f_t) && (9.56)\\ \mathbf{n}(a,0) &= [0, 2\lambda s - 2ba^2] \;\; // \; \mathbf{t} && (9.57)\\ \mathbf{b}(0,b) &= [2\lambda b - 2ab^2, 0] \;\; // \; \mathbf{s} && (9.58) \end{aligned}$$

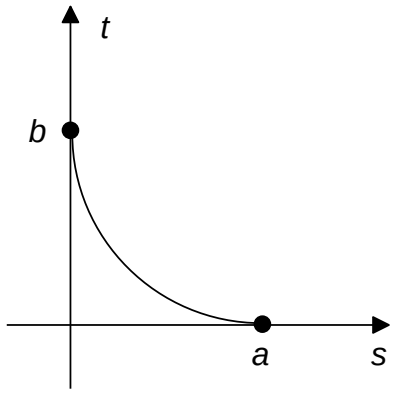

Also,

$$\begin{aligned} f(a,0) &= 2b^2a^2 - 2a^2b^2 = 0 && (9.59)\\ f(0,b) &= 0 && (9.60) \end{aligned}$$

or

$$\begin{aligned} f &= 0 \;\; \text{is tangent to } s \text{ axis at } (a,0) && (9.61)\\ f &= 0 \;\; \text{is tangent to } t \text{ axis at } (0,b) && (9.62) \end{aligned}$$

Theorem: $f(G,H) = 0$ is tangent to $H = 0$ on the curve $G - a = H = 0$, and it is tangent to $G = 0$ on the curve $H - b = G = 0$.

Example: If G, H are quadrics, then the blend is quartic.

Higher order continuity can be achieved by selecting appropriate $f = 0$.

Note: For well-formed "elliptical blend" $-ab < \lambda < ab$ (circle for $a = b$ and $\lambda = 0$).

Applicability: Low order algebraics need ray tracing, and generally lack parametrization.

9.5 Blending as a boundary value problem

9.5.1 Introduction

The motivation for blending surfaces is the need to generate a "secondary" surface as a bridge between primary surfaces, not just for manufacturing purpose, but also for functional, aesthetic, or design purposes. We can view this as a problem where:

- The boundaries are specified;
- The conditions to be met at the boundaries are also specified.

We need to find a smooth surface over some domain that satisfies the boundary conditions. In other words, we want a smoothing or averaging process.

The problem suggests itself as a boundary value problem in which an *elliptic partial differential equation* (*PDE*) needs to be solved subject to imposed boundary conditions. This approach was proposed and developed by Bloor and Wilson and their students at the University of Leeds, UK, [2, 3, 4, 5].

Suppose L is a linear partial differential operator over the domain shown in Figure 9.8.

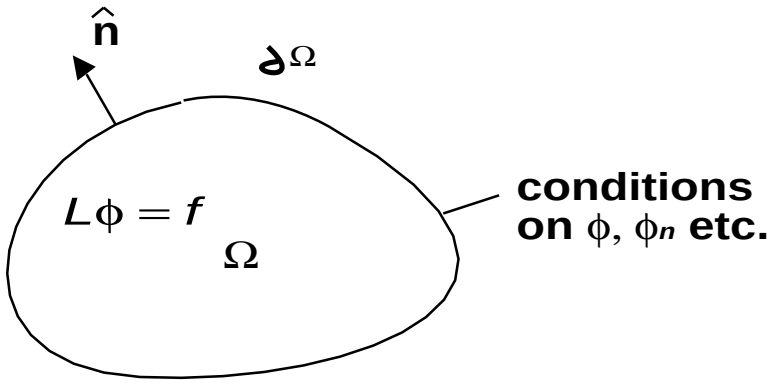

Figure 9.8: Linear partial differential operator.

9.5.2 Example: 2^{nd} order (Laplace) equation

$$\text{(2-D)} \quad \frac{\partial^2 \phi}{\partial x^2} + \frac{\partial^2 \phi}{\partial y^2} \equiv \nabla^2 \phi = 0 \tag{9.63}$$

We can see this as averaging process from analysis.

Analytic approach

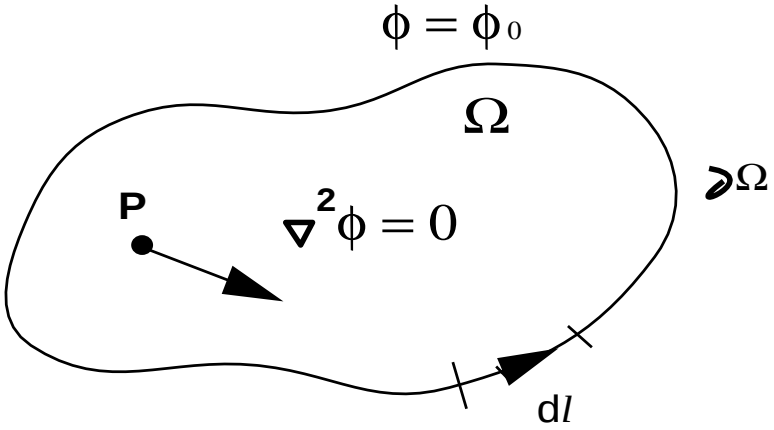

Figure 9.9: Analytic approach.

$$\phi_p = -\frac{1}{2\pi} \int_{\partial\Omega} \frac{\partial \mathcal{G}}{\partial n} \phi_0 d\ell \tag{9.64}$$

where $\phi = \phi_0$ on $\partial\Omega$, $\mathcal{G}$ is the Green's function (source like) that satisfies (see Figure 9.9):

$$\mathcal{G} = 0 \text{ on } \partial\Omega \tag{9.65}$$

Except at P,

$$\partial^2 \mathcal{G} = 0 \quad \text{in} \quad \Omega \tag{9.66}$$

$$\mathcal{G} \sim \ln r \quad \text{at} \quad P \tag{9.67}$$

Numerical approach

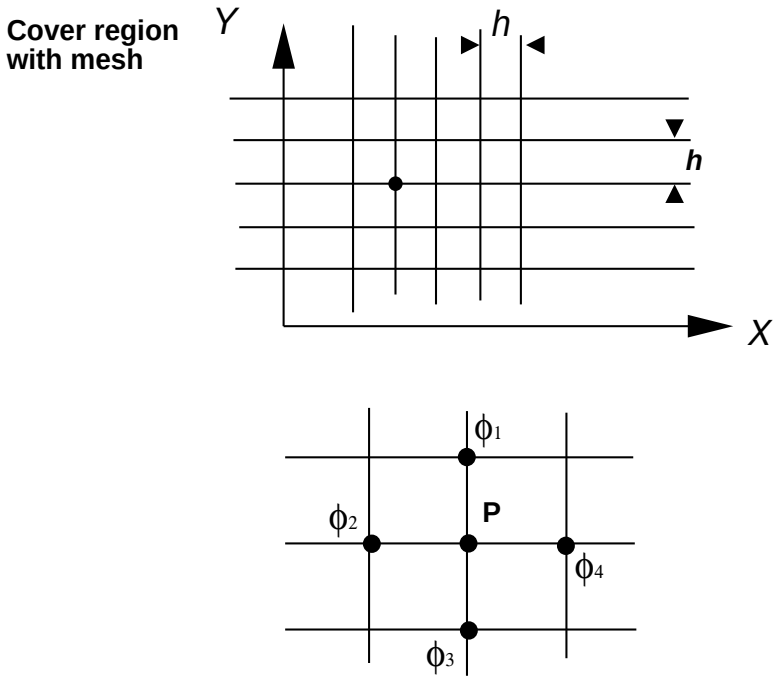

Figure 9.10: Numerical approach.

If we use finite differences to solve Laplace's equation, then (see Figure 9.10):

$$\phi_p = \frac{1}{4}(\phi_1 + \phi_2 + \phi_3 + \phi_4) \tag{9.68}$$

Another example PDE is the 4^{th} order biharmonic equation:

$$\nabla^4 \phi = 0 \tag{9.69}$$

where

$$\nabla^4 \phi = \nabla^2(\nabla^2 \phi) = \phi_{xxxx} + 2\phi_{xxyy} + \phi_{yyyy}$$

which we do not study in these notes.

Numerical Example

We now give a specific numerical example, where x, y are independent variables, z is a dependent variable (ϕ), and $\Omega \quad 0 \leq x \leq 2 : 0 \leq y \leq 2$.

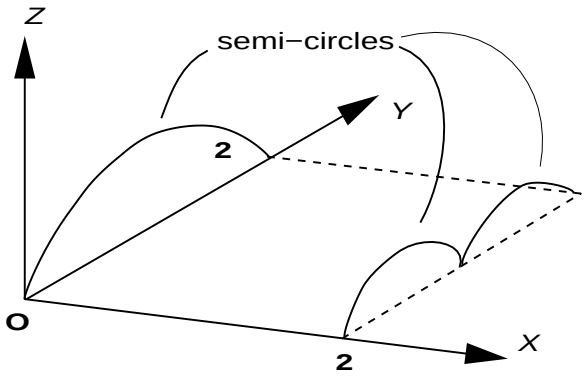

Figure 9.11: Boundary conditions for Laplace equation example.

Boundary conditions - function only (position) because PDE is 2^{nd} order, see Figure 9.11.

$$z = [1 - (1 - y)^2]^{\frac{1}{2}} \qquad x = 0, 0 \leq y \leq 2 \tag{9.70}$$

$$z = [\frac{1}{4} - (y - \frac{1}{2})^2]^{\frac{1}{2}} \qquad x = 2, 0 \leq y \leq 1 \tag{9.71}$$

$$z = [\frac{1}{4} - (y - \frac{3}{2})^2]^{\frac{1}{2}} \qquad x = 2, 1 \leq y \leq 2 \tag{9.72}$$

$$z = 0 \qquad \left.\begin{array}{l} y = 0 \\ y = 2 \end{array}\right\} 0 \leq x \leq 2 \tag{9.73}$$

Limitations:

- inappropriate continuity at boundaries
- multi-valued surfaces would prove difficult (and involve awkward division of region).

Higher order continuity $\Longrightarrow$ higher order PDE. The function and 1st normal derivative $\longrightarrow$ 4^{th} order (tangent plane continuity). The function and 1st and 2nd derivatives $\longrightarrow$ 6^{th} order (curvature continuity).

Rather than use physical coordinates (e.g. x, y) as independent variables, introduce parametric coordinates u, v embedded in the surface with x, y, z as dependent variables.

The surface given parametrically as:

$$\mathbf{x} = \mathbf{x}(u, v) \quad \mathbf{x} = (x, y, z) \tag{9.74}$$

This mapping is determined as a solution to three boundary value problems (one for each coordinate).

Note that this mapping is not given explicitly in terms of polynomials or B-splines.

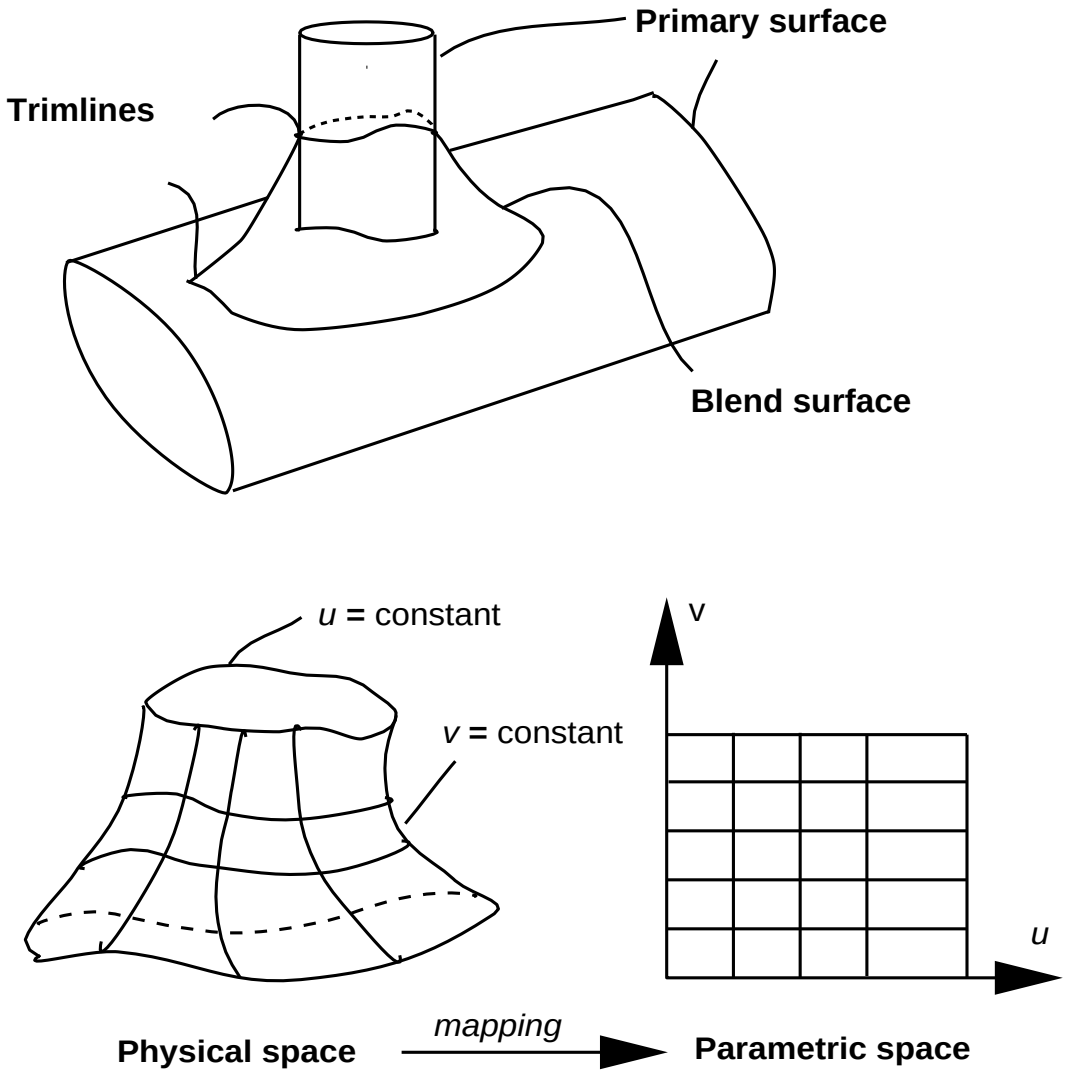

Figure 9.12: Typical blending problem.

9.5.3 Mapping – boundary value problem

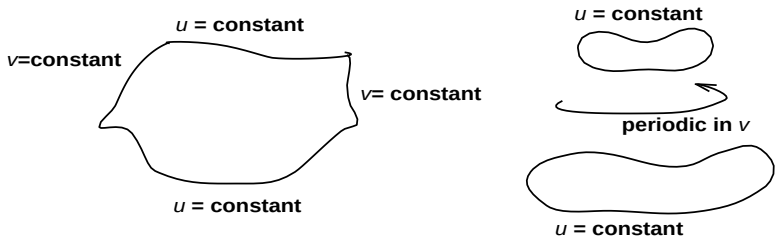

Figure 9.13: Diagrammatic representation of trimlines for non-periodic and periodic cases.

To determine the mapping we need to specify the partial differential equation and the boundary conditions. Both depend on degree of continuity required in the blend.

Position continuity

We specify the value of function $\mathbf{x}$ at the boundary. Hence, we require 2nd order PDE. Consider a modification of the Laplacian operator:

$$\mathcal{D}^2 = \frac{\partial^2}{\partial u^2} + a^2 \frac{\partial^2}{\partial v^2} \tag{9.75}$$

At this stage, restrict a to be a constant. This parameter controls relative "smoothing." To obtain the surface in parametric form (mapping), solve:

$$\mathcal{D}^2 \mathbf{x} = 0 \tag{9.76}$$

(zero RHS in u, v space (Ω) at this stage) subject to $\mathbf{x}$ given on boundary $\partial\Omega$.

Example

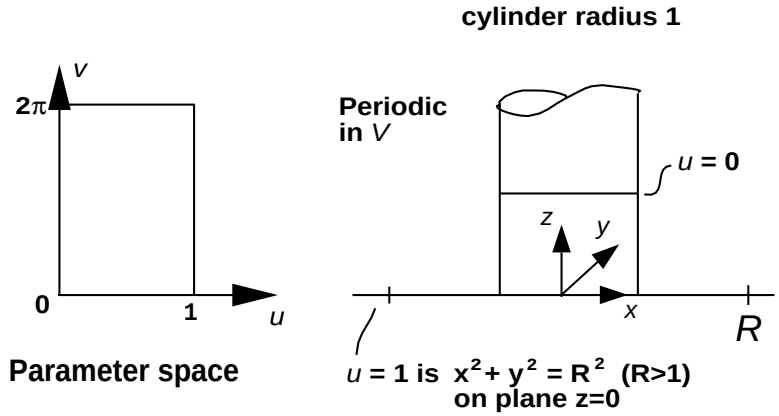

Figure 9.14: Cylinder and plane blending using PDE method.

We need $\mathbf{x}$ as a function of v on the trimlines. Parameterize on arc length:

$$\mathbf{x}(0,v) = \begin{pmatrix} \cos v \\ \sin v \\ H \end{pmatrix} \quad \mathbf{x}(1,v) = \begin{pmatrix} R\cos v \\ R\sin v \\ 0 \end{pmatrix} \tag{9.77}$$

Solution by separation of variables:

$$\mathbf{x} = \begin{pmatrix} \left[\cosh au + \frac{R-\cosh a}{\sinh a}\sinh au\right]\cos v \\ \left[\cosh au + \frac{R-\cosh a}{\sinh a}\sinh au\right]\sin v \\ H(1-u) \end{pmatrix} \tag{9.78}$$

Effect of a

For small a (see Figure 9.15):

$$[\cosh au + \frac{R-\cosh a}{\sinh a}\sinh au] \sim 1 + (R-1)u + O(a^2) \tag{9.79}$$

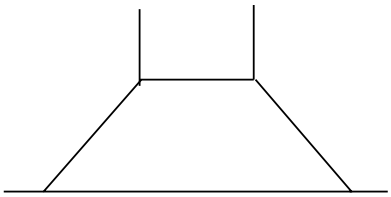

Figure 9.15: Effect of small a.

For large a (see Figure 9.16):

$$[\cosh au + \frac{R-\cosh a}{\sinh a}\sinh au] \sim e^{-au} + Re^{a(u-1)} + O(e^{-a}) \tag{9.80}$$

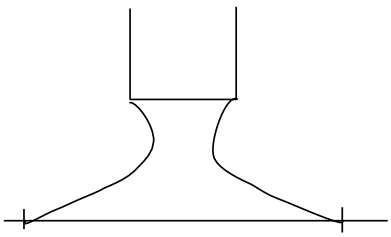

Figure 9.16: Effect of large a.

Note that for some value of a, the blend is tangent to the cylinder. In fact, this occurs for $R = \cosh a$.

Figure 9.17: Blends between circular cylinder and inclined plane, with continuity of slope between blend and primary surfaces. Adapted from Bloor and Wilson [2]

9.5.4 Position and tangent plane continuity

We know the value of the function $\mathbf{x}$ at the boundary and also we know the normal to the surface at the boundary. With $\mathbf{x} = \mathbf{x}(u, v)$ the normal is $\mathbf{x}_u \times \mathbf{x}_v$. Hence we impose a normal derivative condition at the boundary in u, v space.

Hence, we use a 4th order PDE.

In particular, solve

$$D^4\mathbf{x} = 0 \quad \text{in } \Omega \tag{9.81}$$

with

$$\mathbf{x} = \mathbf{x}_o \quad \text{on } \partial\Omega \tag{9.82}$$

$$\mathbf{x}_n = \mathbf{x}_{no} \quad \text{on } \partial\Omega \tag{9.83}$$

where $\mathbf{x}_n$ is the directional partial derivative of $\mathbf{x}$ in the direction normal to the boundary, see Figure 9.18.

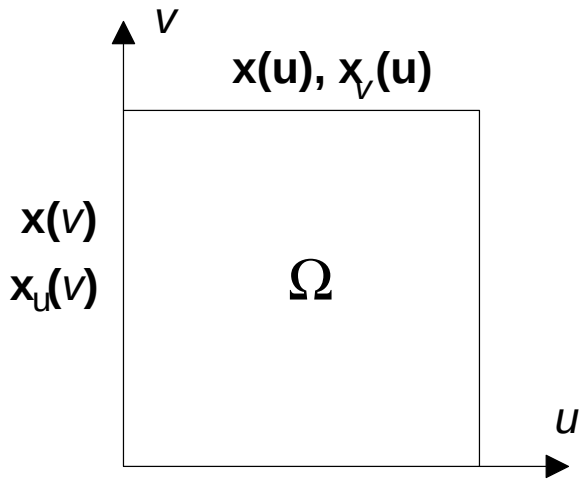

Figure 9.18: Normal derivative condition at the boundary.

9.5.5 Curvature continuity

Surface curvature continuity has been studied theoretically, see Pegna and Wolter [13].

Pegna and Wolter derive a criterion for guaranteeing second-order smoothness or curvature continuity for blending surfaces. Curvature continuity across a linkage curve generally means that the normal curvatures agree in every direction at every point along the linkage curve. They prove the *Linkage Curve Theorem* which states that two surfaces joined with first-order or tangent plane continuity along a first-order continuous linkage curve can be shown to be second-order smooth if the normal curvatures on each surface agree in one direction other than the tangent direction to the linkage curve, see Figure 9.19.

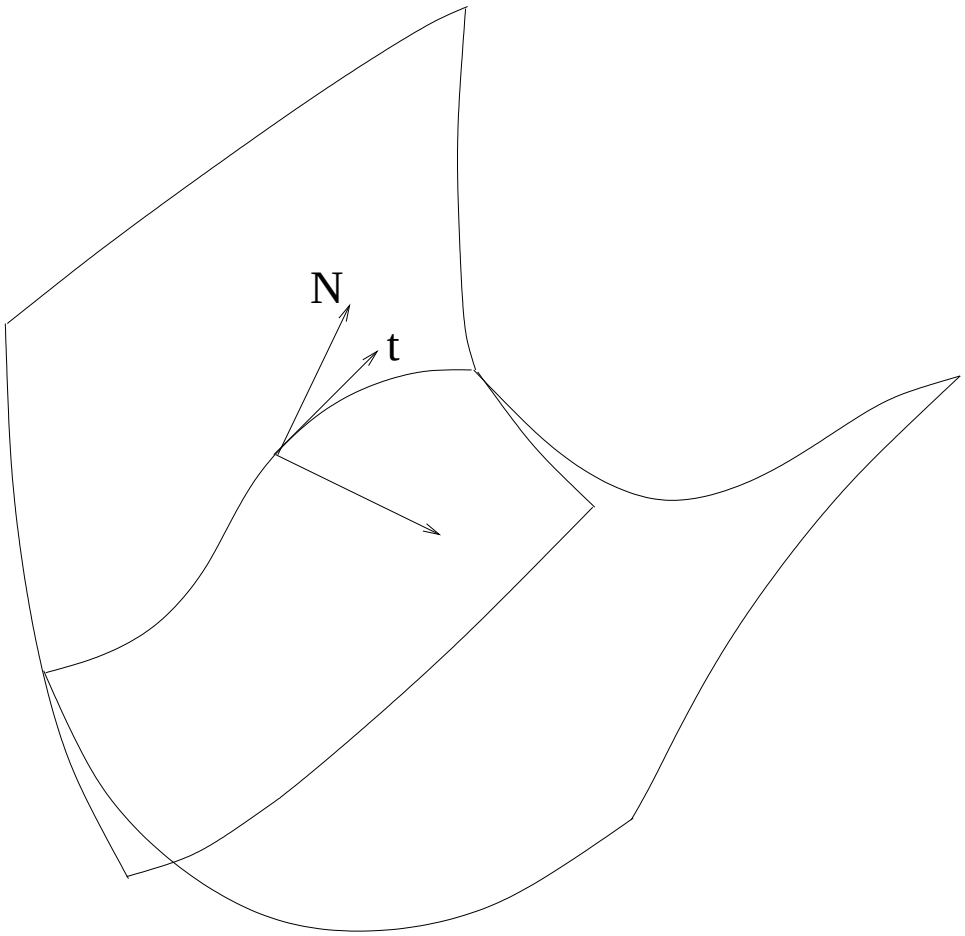

Figure 9.19: Condition for curvature continuity

For a detailed review and a blending surface algorithm for G^1 and G^2 continuity, see Filkins [6].

9.5.6 Multisided blending surfaces

Blending surfaces do not have to be topologically quadrilateral in shape. The following figures illustrate these general blending surfaces.

Figure 9.20: Blends in geometric modelling [15]

Figure 9.21: Generating n-sided patches with partial differential equations [2]

Bibliography

[1] L. Bardis and N. M. Patrikalakis. Blending rational B-spline surfaces. In *Eurographics '89, European Computer Graphics Conference and Exhibition*, pages 453–462, Hamburg, F. R. of Germany, September 1989.

[2] M. I. G. Bloor and M. J. Wilson. Generating blend surfaces using partial differential equations. *Computer-Aided Design*, 21(3):165–171, 1989.

[3] M. I. G. Bloor and M. J. Wilson. Representing pde surfaces in terms of b-splines. *Computer-Aided Design*, 22(6):324–330, July/August 1990.

[4] M. I. G. Bloor and M. J. Wilson. Local control of surfaces generated as the solutions to partial differential equations. *Computers and Graphics*, 18(2):161–169, 1994.

[5] M. I. G. Bloor, M. J. Wilson, and H. Hagen. The smoothing properties of variational schemes. *Computer Aided Geometric Design*, 12(4):381–394, 1995.

[6] P. C. Filkins, S. T. Tuohy, and N. M. Patrikalakis. Computational methods for blending surface approximation. *Engineering with Computers*, 9(1):49–61, 1993.

[7] W. Hansmann. *Interaktiver entwurf und geometrische Beschreibung Glatter Übergänge zwischen räumlich gekrümmten Flächenstrukturen*. PhD thesis, University of Hamburg, Germany, 1985.

[8] C. Hoffmann and J. Hopcroft. The potential method for blending surfaces and corners. In *Geometric Modeling: Algorithms and New Trends*, pages 347–365. SIAM, 1987.

[9] J. Hoschek and D. Lasser. *Fundamentals of Computer Aided Geometric Design*. A. K. Peters, Wellesley, MA, 1993. Translated by L. L. Schumaker.

[10] T. Maekawa. An overview of offset curves and surfaces. *Computer-Aided Design*, 31(3):165–173, March 1999.

[11] T. Maekawa, W. Cho, and N. M. Patrikalakis. Computation of self-intersections of offsets of Bézier surface patches. *Journal of Mechanical Design, Transactions of the ASME*, 119(2):275–283, June 1997.

[12] J. Pegna. *Variable Sweep Geometric Modeling*. PhD thesis, Stanford University, Stanford, CA, 1987.

[13] J. Pegna and F. E. Wolter. Geometrical criteria to guarantee curvature continuity of blend surfaces. *Journal of Mechanical Design, Transactions of the ASME*, 114(1):201–210, March 1992.

[14] J. Pegna and F.-E. Wolter. Surface curve design by orthogonal projection of space curves onto free-form surfaces. *Journal of Mechanical Design, ASME Transactions*, 118(1):45–52, March 1996.

[15] J. R. Woodwark. Blends in geometric modelling. In R. R. Martin, editor, *The Mathematics of Surfaces II*, pages 255–297. Clarendon Press, Oxford, 1987.